

FREEZE-OUT CONFIGURATION PROPERTIES IN
THE $^{197}\text{Au}+^{197}\text{Au}$ REACTION AT 23 AMeV*

R. NAJMAN, R. PŁANETA

The Marian Smoluchowski Institute of Physics, Jagiellonian University
Reymonta 4, 30-059 Kraków, Poland

A. SOCHOCKA

Department of Physics, Astronomy and Applied Informatics
Jagiellonian University
Reymonta 4, 30-059 Kraków, Poland*(Received December 23, 2013)*

We present the results of the experiment performed by the CHIMERA Collaboration with the 4π CHIMERA array, for the system $^{197}\text{Au}+^{197}\text{Au}$ at 23 AMeV. Conclusions related to the shape of the freeze-out configuration are drawn.

DOI:10.5506/APhysPolB.45.475

PACS numbers: 25.70.Jj, 25.70.-z

1. Introduction

The search for exotic nuclear configurations was inspired by Wheeler [1]. His idea was investigated by many authors who studied the stability of exotic nuclear shapes (see *e.g.* [2]). Theoretical investigations related to the synthesis of long-living nuclei beyond the island of stability have shown that they can be reached only if noncompact shapes are taken into account. Calculations for bubble structures showed that such nuclei can be stable for $Z > 240$ and $N > 500$ (see *e.g.* [3]). Recently, it was found that for nuclei with $Z > 140$ the global energy minimum corresponds to toroidal shapes [4]. In contrast to bubble nuclei, the synthesis of toroidal nuclei is experimentally feasible in collisions between stable isotopes.

To address this issue, simulations were performed for Au+Au collisions in a wide range of incident energies using the BUU code [5]. These calculations indicate that the threshold energy for the formation of toroidal nuclear shapes is located around 23 MeV/nucleon.

* Presented at the XXXIII Mazurian Lakes Conference on Physics, Piaski, Poland, September 1–7, 2013.

In order to study experimentally possible formation of noncompact nuclear systems, the measurements were performed by the CHIMERA Collaboration for the system $^{197}\text{Au}+^{197}\text{Au}$ at 23 AMeV [6].

In this work, we report the results of data analysis. The experimental data are compared with the model predictions. Conclusions related to the shape of the freeze-out configuration are drawn.

This paper is organized as follows. In Sec. 2 we present the experiment and data calibration procedures. Data analysis is shown in Sec. 3. The conclusions are presented in Sec. 4.

2. Experiment and data calibration procedure

The experiment for the Au+Au reaction was performed in March 2010 using the CHIMERA detector [7] at INFN-LNS. Energy calibration of Si detectors was performed using ion beams, delivered both by the tandem and the cyclotron. In our energy calibration of silicon detectors, a pulse-height defect was taken into account by using the same procedure as in [8].

In order to identify fragments, two methods were applied: (i) the $\Delta E-E$ technique for fragments punching through the silicon detectors; (ii) the time-of-flight (TOF) method for the class of fragments stopped in Si detectors. In order to estimate a piece of missing information about mass or charge of the identified fragment, the Charity formula [9] was used.

The mass of fragments stopped in Si detector is determined by TOF method. The start signal was given by 30% Constant Fraction Discriminator acting on time signal generated by the silicon detector, while the stop signal was given by the delayed Reference Signal delivered by cyclotron. In this case, mass values are calculated using the formula

$$m = 2E(t_0 - t)^2/R^2, \quad (1)$$

where R is the distance between the target and a given detector, and the t_0 is a time offset of the measured time t . The values of time offset t_0 are dependent on incident energy and mass of the particle detected in silicon detector (see Fig. 1). In our analysis, this dependence was parametrized by the phenomenological formula

$$t_0 = \text{const} - (b/m + \beta) E \exp[-(c/m + d) E], \quad (2)$$

where the parameters b and c give the mass dependence of the time offset at low energies. The values of the parameters were established in the fitting procedure. Results of the fitting procedure are shown for the telescope number 653 in Fig. 1.

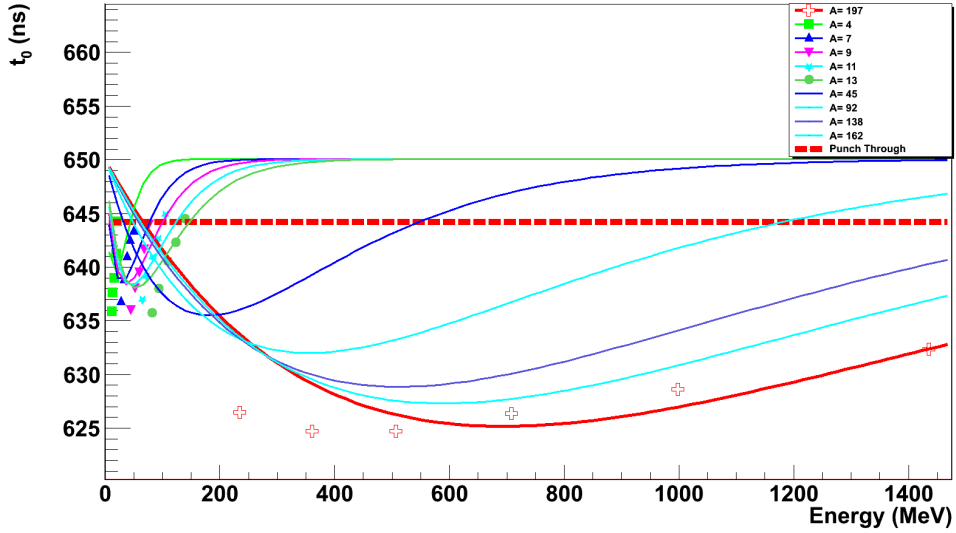


Fig. 1. The t_0 parameter dependence on incident energy and particle mass for telescope number 653 located at $\theta = 28.5^\circ$. Colour symbols represent the t_0 values for identified light fragments and Au-like fragments. Lines represent the fitting results using Eq. (2).

Inserting Eq. (2) into (1) the masses of particles were calculated in the iterative procedure. In frame of this procedure, fragment energies were corrected for pulse height defect and charge values were estimated using the Charity formula [9]. For Au-like nuclei we assigned charge 79.

For the identified fragments ($Z_{\text{frag}} \geq 3$), we have constructed the plot presenting the dependence between the total charge of identified fragments, Z_{tot} , versus total parallel momentum of those fragments normalized to the beam momentum, $p_{\parallel, \text{tot}}/p_{\text{proj}}$ (see Fig. 2). Additionally, the projection of this spectrum on Z_{tot} axis is presented in Fig. 3 for the region of $Z_{\text{tot}} \geq 100$.

One can distinguish different regions in Fig. 2. In the region of total parallel momentum close to 1 and total collected charge close to the charge of the projectile, one observes the maximum corresponding to deep inelastic collisions when the target-like fragment stays undetected. A region where the total detected charge is close to the total charge of the system and the total parallel linear momentum is close to the linear momentum of the projectile can be called as the region of well defined events. In our present analysis, this region is delimited by the conditions

$$120 < Z_{\text{tot}} < 180 \quad \text{and} \quad 0.8 < p_{\parallel, \text{tot}}/p_{\text{proj}} < 1.1. \quad (3)$$

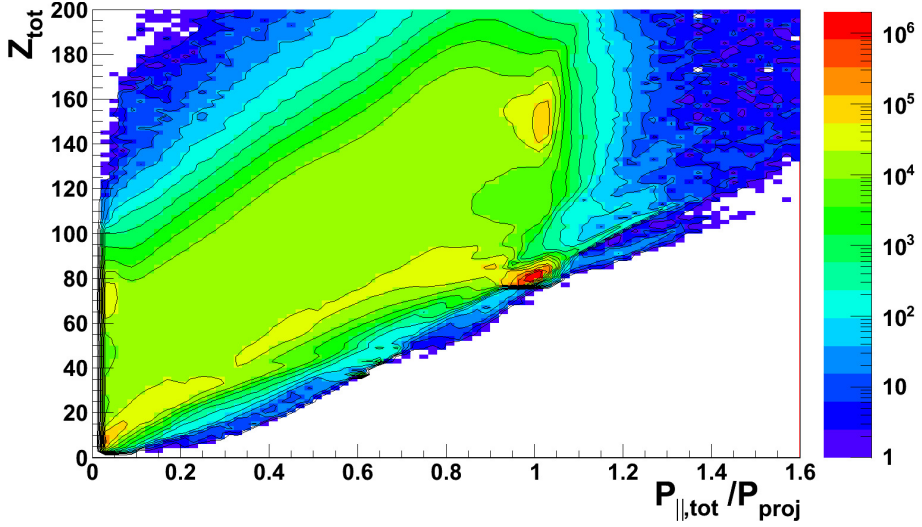


Fig. 2. The correlation between total charge of identified fragments *versus* total parallel momentum of those fragments normalized to the beam momentum.

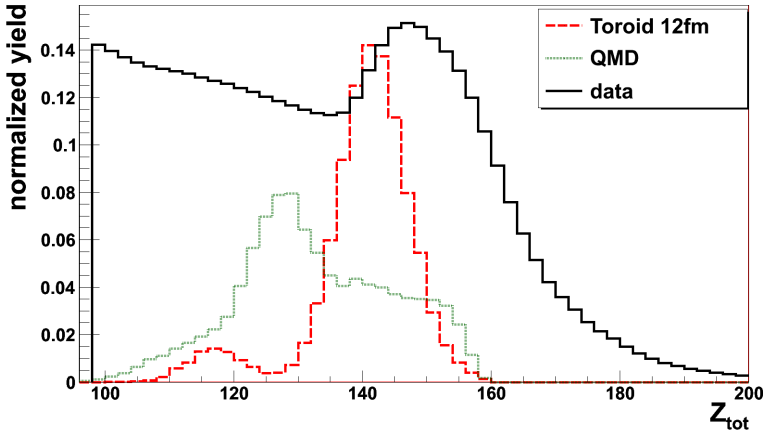


Fig. 3. The total charge of identified fragments for experimental data and Toroid 12 fm and QMD model predictions (see Sec. 3).

3. Data analysis

For the class of events with five fragments, one can consider at least two mechanisms responsible for the presence of the fifth heavy fragment: *(i)* creation of the fragment in the interaction region (intermediate velocity source) for more peripheral collisions or *(ii)* the multifragmentation of the composite nuclear system formed in central collisions.

In order to investigate the reaction scenario responsible for events with five fragments, we have compared experimental data with the ETNA and QMD model predictions. The ETNA model can simulate the decay of nuclear system assuming compact and noncompact freeze-out configurations [10]. In this model, three freeze-out configurations are considered: (i) ball geometry with volume 3 and 8 times larger than the normal nuclear volume (fragments uniformly distributed inside the sphere); (ii) fragments distributed on the surface of the sphere mentioned above (bubble configuration); (iii) fragments distributed on the ring with diameter 12 fm and 15 fm (toroidal configuration). In this model, we consider only events corresponding to central collisions (0–3 fm impact range). In order to simulate the contribution from noncentral collisions the QMD model [11] calculations were performed in the full impact parameter range 0–12 fm. In Fig. 3 the model predictions for Toroid 12 fm configuration and QMD model are compared with Z_{tot} spectrum constructed for experimental data.

In our analysis, we decide to cut out noncentral events both for experimental data and model predictions by using the condition $\theta_{\text{flow}} > 20^\circ$ [12]. In order to disentangle different freeze-out configuration predictions of the ETNA and QMD models, several observables were investigated. We use dedicated observables sensitive to the shape of freeze-out configurations: δ and Δ^2 [10]. The δ variable is related to sphericity and coplanarity variables. In Fig. 4 (left panels), the δ distribution for experimental data is compared with the ETNA model predictions for Ball $8V_0$, Bubble $8V_0$ freeze-out geometries and QMD predictions (upper left panel). In the bottom left panel, experimental distribution is compared with predictions for Toroid 12 fm and Toroid 15 fm geometries. One can see here that the δ distribution for experimental data is similar to that corresponding to the toroidal configurations and QMD predictions.

The Δ^2 variable used in our analysis gives a measure of the event flatness in the velocity space. For each event, we are establishing the plane in the velocity space. The parameters of this plane are selected in the way that the sum of squares of distances between the plane and the endpoints of velocity vectors reach the minimum value. This quantity is defined as

$$\Delta^2 = \min \left[\sum_{i=1}^5 (d_i^2(A, B, C, D)) \right], \quad (4)$$

where

$$d_i = \frac{A v_{x,i} + B v_{y,i} + C v_{z,i} + D}{\sqrt{A^2 + B^2 + C^2}}. \quad (5)$$

The parameters A, B, C, D are the plane parameters and the velocities of fragments are in the velocity of light units.

The corresponding distributions are shown in Fig. 4 (right panels) for data and model predictions. One can see here that for Δ^2 variable the biggest difference between experimental distribution and model predictions is observed for the Ball $8V_0$, and Bubble $8V_0$ configurations.

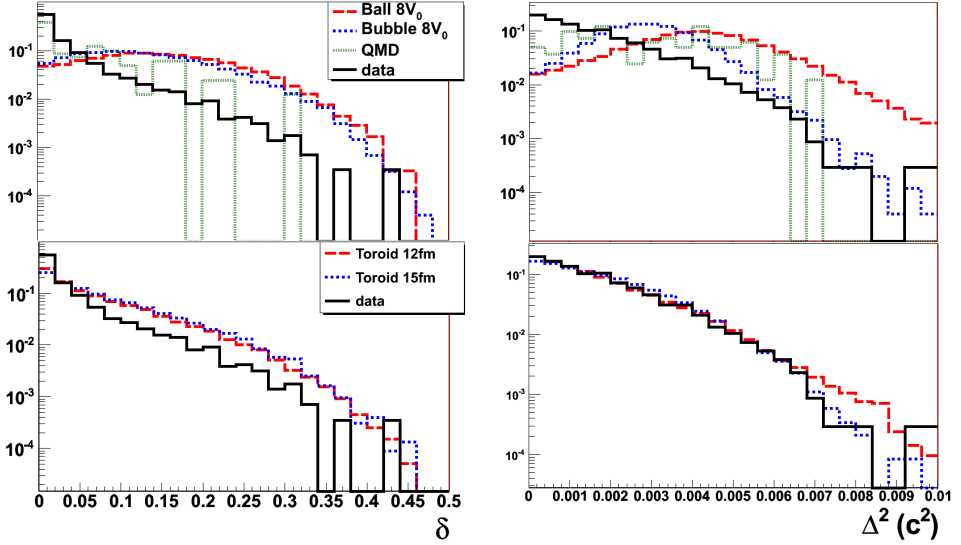


Fig. 4. The δ distributions (upper left panel) are presented for experimental data, Ball $8V_0$, Bubble $8V_0$ freeze-out geometries, and QMD predictions. In the bottom left panel, the experimental distribution is compared with predictions for Toroid 12 fm and Toroid 15 fm configurations. In the right panels, the Δ^2 distributions for experimental data and model predictions are shown. All the distributions presented here are constructed using the condition $Z_{\text{frag}} \geq 10$.

In conjecture with Δ^2 parameter, one can define an angle, θ_{plane} , between the beam direction and vector normal to the plane defined by parameters A , B , C , and D . For events corresponding to noncentral collisions, where most of reaction products are located in the reaction plane, θ_{plane} should be close to 90° . For toroidal freeze-out configurations predicted by BUU calculations this angle should be significantly smaller. In order to reduce remaining contribution of noncentral collisions, we use additional condition $\theta_{\text{plane}} < 75^\circ$.

Following the method proposed in Ref. [10], we select events corresponding to the toroidal shape by the set of conditions

$$\Delta^2 < 0.001 \, c^2 \quad \text{and} \quad \delta < 0.05. \quad (6)$$

As an efficiency measure of the above conditions, we take the ratio of the number of events fulfilling the selection conditions to the number of events with 5 heavy fragments (efficiency factor, EF). The results of this procedure are listed in Table I.

TABLE I

The efficiency factor at incident energy 23 AMeV for three threshold values of the fragment charge.

Configuration	Efficiency factor [%]		
	$Z_{\text{frag}} \geq 3$	$Z_{\text{frag}} \geq 10$	$Z_{\text{frag}} \geq 15$
Ball $3V_0$	3.3 ± 0.2	3.5 ± 0.2	3.5 ± 0.2
Bubble $3V_0$	2.4 ± 0.2	2.6 ± 0.2	2.7 ± 0.2
Ball $8V_0$	3.2 ± 0.2	3.5 ± 0.2	3.5 ± 0.2
Bubble $8V_0$	3.9 ± 0.2	4.6 ± 0.2	4.7 ± 0.2
Toroid 12 fm	29.7 ± 0.6	31.6 ± 0.6	31.8 ± 0.6
Toroid 15 fm	25.2 ± 0.5	27.5 ± 0.5	27.7 ± 0.5
QMD	13.7 ± 3.4	8.2 ± 4.7	6.3 ± 5.5
Data	30.2 ± 0.8	30.4 ± 2.4	26.1 ± 3.5

As one can see, the EF is very low for spherical freeze-out configurations with respect to the corresponding values for toroidal configurations. The EF values for QMD predictions are located between these limits and is dependent on the threshold value of the fragment charge. The EF values for experimental data are very close to the predictions for Toroid 12 fm freeze-out configuration.

4. Summary

In this paper, the results of the measurements performed for Au+Au system at 23 AMeV are presented. Basic information about data calibration procedure are summarized. The bulk properties of the experimental data are shown. The experimental data are compared with the ETNA and QMD model predictions. Efficiency factor is used as an indication of the formation of an exotic freeze-out configuration. Comparison between experimental data and model predictions may indicate the formation of flat/toroidal nuclear systems. The latter observation needs to be verified by a more detailed analysis. This analysis is in progress.

This work has been partly supported by the National Science Centre of Poland (grant N N202 180638) and by the grant of the Polish Ministry of Science and Higher Education number 7150/E-338/M/2013.

REFERENCES

- [1] J.A. Wheeler, *Nucleonic Notebook*, 1950, unpublished.
- [2] P.J. Siemens, H. Bethe, *Phys. Rev. Lett.* **18**, 704 (1967); C.Y. Wong, *Phys. Rev. Lett.* **55**, 1973 (1985); L.G. Moretto *et al.*, *Phys. Rev. Lett.* **78**, 824 (1997).
- [3] K. Dietrich, K. Pomorski, *Phys. Rev. Lett.* **80**, 37 (1998); J.F. Berger *et al.*, *Nucl. Phys.* **A685**, 1 (2001); J. Decharge *et al.*, *Nucl. Phys.* **A716**, 55 (2003).
- [4] M. Warda, *Int. J. Mod. Phys.* **E16**, 452 (2007); A. Staszczak, C.Y. Wong, *Acta Phys. Pol. B* **40**, 753 (2009).
- [5] A. Sochocka *et al.*, *Int. J. Mod. Phys.* **E17**, 190 (2008); A. Sochocka *et al.*, *Acta Phys. Pol. B* **39**, 405 (2008).
- [6] R. Najman *et al.*, *EPJ Web of Conferences* **31**, 00026 (2012).
- [7] A. Pagano *et al.*, *Nucl. Phys.* **A734**, 504 (2004).
- [8] G. Pasquali *et al.*, *Nucl. Instrum. Methods* **A405**, 39 (1998).
- [9] R.J. Charity *et al.*, *Phys. Rev.* **C58**, 1073 (1998).
- [10] A. Sochocka *et al.*, *Acta Phys. Pol. B* **40**, 747 (2009); A. Sochocka, Ph.D. Thesis, Jagiellonian University, 2009, unpublished.
- [11] J. Łukasik, Z. Majka, *Acta Phys. Pol. B* **24**, 1959 (1993).
- [12] J. Cugnon, D. L'Hote, *Nucl. Phys.* **A397**, 519 (1983).